Contribution from the Department of Chemistry,
University of Texas at Dallas, Richardson, Texas 75083-0688

Synthesis and Characterization of a Series of Macrocyclic Chelates Containing O and N Donors: Prospects for Use as NMR Shift Agents for Alkali-Metal Cations

R. Merritt Sink, Douglas C. Buster, and A. Dean Sherry*

Received November 27, 1989

A new series of polyoxa tetraaza macrocyclic tetraacetates have been prepared and characterized. These derivatives chelate lanthanides and transition-metal ions in the tetraaza tetraacetate portion of the macrocycle, leaving the polyoxa portion available for binding with alkali-metal cations. The protonation constants and metal-binding properties of these chelates have been investigated and compared to those of the parent molecule 1,4,7,10-tetraazacyclododecane-1,4,7,10-tetraacetic acid (DOTA). Molecular mechanics calculations were performed to estimate the polyoxa cavity sizes, and these results were compared to those of the crown ether series. The Dy^{3+}, Ni^{2+}, and Co^{2+} complexes were examined for their ability to induce a paramagnetic shift in the $^{23}Na^+$ NMR resonance of aqueous NaCl at pH 7. The Dy^{3+} complex formed with the tetraoxa tetraaza macrocycle (O_4N_4) produced the largest ^{23}Na paramagnetic shift, opposite in direction to that produced by $Dy(DOTA)^-$. This verified that Na^+ (and other alkali-metal cations) binds in the polyoxa cavity, orthorogonal to the presumed symmetry axis of the Dy^{3+} cation bound within the tetraaza tetraacetate portion of the macrocycle. Competitive titrations with Ca^{2+} indicate that these ligands are considerably more specific for Na^+ ions than are the more common ion-pairing ^{23}Na shift agents.

Introduction

Water-soluble anionic paramagnetic shift reagents[1-3] now make it possible to distinguish intra- and extracellular cations by NMR spectroscopy in a variety of intact cells and tissues. Three shift reagent (SR) systems have so far proven to be most promising: dysprosium(III) bis(tripolyphosphate) ($Dy(PPP)_2^{7-}$), dysprosium(III) triethylenetetraminehexaacetic acid ($Dy(TTHA)^{3-}$), and more recently the dysprosium(III)[4] and thulium(III)[5] complexes of 1,4,7,10-tetraazacyclododecane-1,4,7,10-tetrakis(methylenephosphonate) (DOTP). One of the main problems with these SRs is their nonspecificity for a particular biological cation such as Na^+. In virtually all cases, competitive binding of other cations present in physiological solutions decreases the $^{23}Na^+$ induced shift. Especially problematic are the divalent cations Mg^{2+} and Ca^{2+}. Calcium complexation can be particularly severe, sometimes resulting in the release of free lanthanide cations by competition or in the precipitation of binary SR-calcium complexes.[6,7] Furthermore, the removal of free calcium from solution by complexation or precipitation may often have a detrimental effect upon those tissues which depend upon low Ca^{2+} concentrations for survival.

To explore the possibility of making SRs that are more specific for certain cations, a new series of polyoxa tetraaza macrocyclic tetraacetates have been prepared. The tetraaza tetraacetate portion of the molecule is similar to tetraazacyclododecanetetraacetic acid (DOTA) and houses the paramagnetic cation, leaving the polyoxa cavity available for binding to alkali-metal cations. The macrocycles prepared contain a variable number of oxygens (see I) in the polyoxa cavity. Cavity sizes for this series of SRs were estimated by using molecular mechanics methods and compared to the crown ether series. Paramagnetic shifts were measured for a series of alkali-metal cations in the presence of the Dy^{3+}-macrocycle complexes, and competition between Na^+ and Ca^{2+} for binding to one of the macrocycles was compared to similar results for other commonly used sodium SRs.

Experimental Section

General Procedures. NMR spectra were recorded on either a General Electric GN-500 or a JEOL JNM-FX200 NMR spectrometer. Infrared spectra were taken on a Nicolet 5DX FT-IR spectrophotometer, and melting points were determined by using a Thomas Hoover capillary melting point apparatus. Potentiometric titrations were performed by using a Brinkmann 665 Dosimat auto titrator and a Corning 250 pH meter equipped with an Orion 8103 Ross combination pH electrode. Elemental analyses were performed by either Galbraith Laboratories, Inc., or Oneida Research Services, Inc. Mass spectral data were obtained at the Midwest Center for Mass Spectrometry, University of Nebraska—Lincoln.

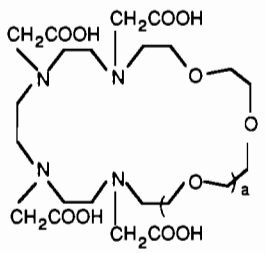

O_3N_4 (a=1)
O_4N_4 (a=2)
O_5N_4 (a=3)
O_6N_4 (a=4)

I

1,4,7,10-Tetratosyl-1,4,7,10-tetraazadecane was prepared by the method of Koyama and Yoshino.[8] 1,14-Ditosyl-3,6,9,12-tetraoxatetradecane was purchased from Aldrich Chemical Co. The remaining ditosylpolyoxanes were prepared and characterized by methods similar to those reported previously.[9]

Synthesis of the Tetratosyl Polyoxa Tetraaza Macrocycles. 1,4,7,10-Tetratosyl-1,4,7,10-tetraazadecane (1.23 mmol) and Cs_2CO_3 (3.69 mmol) were placed into a 250-mL three-neck round-bottom flask containing 31 mL of dry dimethylformamide (DMF). The DMF solution was stirred under nitrogen for 1 h at 65 °C. In a separate flask, 1.23 mmol of the appropriate ditosylpolyoxane was mixed with 30 mL of dry DMF. The ditosylpolyoxane solution was added dropwise over the course of 4 h to the reaction flask. After the addition was complete, the mixture was stirred under nitrogen at 65 °C for 4 days and the progress of the reaction was followed by thin-layer chromatography using 5% methanol in methylene chloride. DMF was removed by rotary evaporation, leaving an orange, oily residue. Each of the four oily residues was dissolved into methylene chloride (CH_2Cl_2), isolated as a solid, and characterized as follows.

10,13,16,19-Tetratosyl-1,4,7-trioxa-10,13,16,19-tetraazacycloheneicosane was isolated as a white solid from CH_2Cl_2 and recrystallized from CH_3CN (75.0% yield): mp 191-192 °C (lit.[10] 192-193 °C); ^1H NMR δ 2.42 (s, 6 H), 2.44 (s, 6 H), 3.25-3.54 (m, 28 H), 7.31 (t, 8 H), 7.72 (t, 8 H); ^{13}C NMR δ 21.47, 49.20, 49.55, 50.14, 69.58, 70.17, 70.46, 127.22, 127.52, 129.68, 135.05, 135.93, 143.46. Anal. Calcd for

(1) Gupta, R. J.; Gupta, P. *J. Magn. Reson.* **1982**, *47*, 344.
(2) Pike, M. M.; Springer, C. S., Jr. *J. Magn. Reson.* **1982**, *46*, 348.
(3) Balschi, J. A.; Cirillo, V. P.; Springer, C. S., Jr. *Biophys. J.* **1982**, *38*, 323.
(4) Sherry, A. D.; Malloy, C. R.; Jeffery, F. M. H.; Cacheris, W. P.; Geraldes, C. F. G. C. *J. Magn. Reson.* **1988**, *76*, 528.
(5) Buster, D. C.; Castro, M. M. C. A.; Geraldes, C. F. G. C.; Malloy, C. R.; Sherry, A. D.; Siemers, T. C. *Magn. Reson. Med.* **1990**, *15*, 25.
(6) Seo, Y.; Murakami, M.; Matsumoto, T.; Nishikawa, H.; Watari, H. *J. Magn. Reson.* **1987**, *72*, 341.
(7) Springer, C. S., Jr. In *NMR Techniques in the Study of Cardiovascular Structure and Function*; Osbakken, M., Haselgrove, J., Eds.; Futura Publishing Co.: New York, 1988; Chapter 14.
(8) Koyama, H.; Yoshino, T. *Bull. Chem. Soc. Jpn.* **1972**, *45*, 481.
(9) Searle, G. H.; Geue, R. J. *Aust. J. Chem.* **1984**, *37*, 959.
(10) Rasshofer, W.; Wehner, W.; Vogtle, F. *Justus Liebigs Ann. Chem.* **1976**, 916.

0020-1669/90/1329-3645$02.50/0

$C_{42}H_{56}N_4S_4O_{11}$: C, 54.78; H, 6.09; N, 6.09; S, 13.91; O, 19.13. Found: C, 54.52; H, 5.95; N, 6.09; S, 13.96. Mass spectrometry showed the molecular ion at m/z 921 (lit.[10] m/z 921).

13,16,19,22-Tetratosyl-1,4,7,10-tetraoxa-13,16,19,22-tetraazacyclotetracosane crystallized from CH_2Cl_2 following silica-gel chromatography (70.0% yield): mp 180–182 °C (lit.[11] 179–185 °C); ^{1}H NMR δ 2.41 (s, 6 H), 2.43 (s, 6 H), 3.34–3.55 (m, 32 H), 7.29 (t, 8 H), 7.72 (m, 8 H); ^{13}C NMR δ 21.46, 48.33, 48.62, 49.73, 70.11, 70.46, 71.28, 127.11, 127.46, 129.68, 135.63, 136.33, 143.22, 143.34. Anal. Calcd for $C_{44}H_{60}N_4S_4O_{12}$: C, 54.77; H, 6.22; N, 5.81; O, 19.92; S, 13.28. Found: C, 54.47; H, 6.35; N, 5.65; O, 19.91. Mass spectrometry showed the molecular ion at m/z 965 (lit.[11] m/z 965).

16,19,22,25-Tetratosyl-1,4,7,10,13-pentaoxa-16,19,22,25-tetraazacycloheptacosane crystallized as a white solid following silica-gel chromatography (60.0% yield): mp 108–110 °C (lit.[10] 192–194 °C; we are in disagreement with the published melting point value); ^{1}H NMR δ 2.40 (s, 6 H), 2.43 (s, 6 H), 3.34–3.55 (m, 36 H), 7.31 (t, 8 H), 7.74 (t, 8 H); ^{13}C NMR δ 21.46, 48.66, 48.91, 49.48, 50.37, 70.36, 71.12, 127.10, 127.61, 129.69, 135.20, 136.09, 143.30. Anal. Calcd for $C_{46}H_{64}N_4S_4O_{13}$: C, 54.76; H, 6.35; N, 5.56; O, 20.63; S, 12.70. Found: C, 54.80; H, 6.31; N, 5.47; O, 20.51. Mass spectrometry showed the molecular ion at m/z at 1009 (lit.[10] m/z 1009.3).

19,22,25,28-Tetratosyl-1,4,7,10,13,16-hexaoxa-19,22,25,28-tetraazacyclotriacontane crystallized as a white solid following chromatography (30.0% yield). There was a problem with the formation of the dimer in this reaction. However, the two compounds were easily separated by silica-gel chromatography: mp 140–141 °C; ^{1}H NMR δ 2.40 (s, 6 H), 2.42 (s, 6 H), 3.33–3.59 (m, 40 H), 7.30 (t, 8 H), 7.75 (t, 8 H); ^{13}C NMR δ 21.52, 49.14, 49.96, 70.23, 70.46, 127.28, 127.57, 129.74, 135.28, 136.04, 143.28, 143.46. Anal. Calcd for $C_{48}H_{68}N_4S_4O_{14}$: C, 54.75; H, 6.46; N, 5.32; O, 21.29; S, 12.17. Found: C, 54.94; H, 6.52; N, 5.18; O, 21.13. Mass spectrometry showed the molecular ion at m/z 1053.

Synthesis of the Polyoxa Tetraaza Tetraacetic Acids. Each fully characterized tosylated macrocycle was converted to the corresponding free amine by using 3% Na/Hg amalgam in refluxing methanol, as reported previously,[11,12] with yields ranging from 82 to 91%. Then, in a typical procedure, 0.807 mmol of the tetratosyl polyoxa tetraaza macrocycle were dissolved into 10 mL of water plus enough acetonitrile to solubilize the free amine. In a separate flask, 3.23 mmol of bromoacetic acid was dissolved in 5 mL of deionized water, and the solution was stirred and cooled to 5 °C in an ice–water bath. A stoichiometric amount of NaOH (in 5 mL of water) was added dropwise to the solution. The neutralized bromoacetic acid was warmed to room temperature and added to the amine. The solution was heated to 80 °C, and the pH (monitored by using a pH electrode) was maintained in the range of 9–10.2 by adding an additional stoichiometric amount of NaOH. The reaction was complete after all of the NaOH was added. The sample was neutralized (pH 7) and rotary-evaporated, leaving an oil residue. Small amounts of excess bromoacetic acid were removed by using a Dowex 1 ion-exchange column.[13] A final purification of the tetraacetate salt was carried out by using Dowex 50 (chloride form; 200–400 mesh) ion-exchange chromatography and a hydrochloric acid gradient (0–0.1 M) in water. The eluates were combined and rotary-evaporated. Each of the four products was isolated as a white solid following lyophilization.

1,4,7-Trioxa-10,13,16,19-tetraazacycloheneicosane-10,13,16,19-tetraacetic acid (O_3N_4) was isolated as a hygroscopic solid in 50.0% yield. The ^{1}H NMR spectrum of the product was too complex for complete characterization, but integration of the ^{13}C NMR spectrum (measured under nonsaturating conditions and without a nuclear Overhauser enhancement) verified that the macrocycle contained exactly four acetates: ^{13}C NMR δ 50.21, 51.48, 51.79, 54.83, 55.78, 64.44, 69.82, 70.26, 169.71, 172.30.

1,4,7,10-Tetraoxa-13,16,19,22-tetraazacyclotetracosane-13,16,19,22-tetraacetic acid (O_4N_4) was isolated as a white, hygroscopic solid in 56.0% yield: FT-IR (neutral salt) 1638 and 1598 cm^{-1} (COO^-), 1212 cm^{-1} (C–O); ^{1}H NMR too broad for identification; ^{13}C NMR δ 49.87, 51.52, 54.68, 55.17, 64.35, 69.82, 70.07, 168.95, 172.17.

1,4,7,10,13-Pentaoxa-16,19,22,25-tetraazacycloheptacosane-16,19,22,25-tetraacetic acid (O_5N_4) was isolated as a white, hygroscopic solid in 60.0% yield: ^{1}H NMR too broad for identification; ^{13}C NMR δ 50.21, 51.67, 54.96, 55.71, 64.44, 69.82, 169.27, 172.30.

1,4,7,10,13,16-Hexaoxa-19,22,25,28-tetraazacyclotriacontane-19,22,25,28-tetraacetic acid (O_6N_4) was isolated as a white, hygroscopic solid in 61.7% yield: ^{1}H NMR too broad for identification; ^{13}C NMR δ 49.61, 51.26, 51.54, 54.58, 54.96, 64.26, 69.44, 69.67, 168.53, 171.88.

(11) Sessler, J. L.; Sibert, J. W.; Hugdahl, J. D.; Lynch, V. *Inorg. Chem.* **1989**, *28*, 1417.
(12) Vriesema, B. K.; Buter, J.; Kellogg, R. M. *J. Org. Chem.* **1984**, *49*, 110.
(13) Desreux, J. F. *Inorg. Chem.* **1980**, *19*, 1319.

Table I. Protonation Constants[a] Determined by Potentiometry in 0.1 M Tetramethylammonium Chloride (25 °C)

	log K_1	log K_2	log K_3	log K_4
O_3N_4	11.09	9.04	5.10	2.70
O_4N_4	11.50	9.11	5.17	2.69
O_5N_4	11.54	9.03	5.21	2.83
O_6N_4	11.60	9.02	5.16	2.70
DOTA[b]	12.09	9.68	4.55	4.13

[a] Standard deviations are $\leq \pm 0.6$ ($n = 3$). [b] Reference 20.

Potentiometric Titrations. The hydrogen ion concentration was calculated from the measured pH values by using a procedure reported by Irving et al.[14] The pH electrode was calibrated with standard Fisher pH 4 and 7 buffers. Standardized solutions of each polyoxa tetraaza macrocyclic tetraacetic acid containing 0.1 M tetramethylammonium chloride to maintain constant ionic strength were titrated at 25 °C against standardized 0.1 M KOH. (In the case of stability constant determinations, only equimolar ligand–metal complexes were evaluated.) The protonation and thermodynamic stability constants were calculated by entering the corrected pH values versus the volume of titrant added along with the K_w into two different BASIC programs[15] (stability measurements used the pH range of 2.0–6.6). These programs utilize a Simplex algorithm that calculates the best fit, nonlinear regression for determination of the protonation and stability constants.

Molecular Mechanics. To evaluate the polyoxa cavity sizes of these ligands bound with dysprosium, calculations were performed by using MM2 force field[16] molecular mechanics techniques.[17,18] Since MM2 parameters for the lanthanides do not exist, crystallographic data[19] from $Eu(DOTA)^-$ were initially used to model the $Dy(DOTA)^-$ complex. From the minimized $Dy(DOTA)^-$ model, the polyoxa functionalities were added and minimized for estimations of the lowest energy conformation of each of the complexes. Because of the possibility of local minimum geometries, different conformations for the polyoxa portion of these complexes were entered to find the true minimized structure.

NMR Spectroscopy. ^{7}Li, ^{23}Na, and ^{133}Cs NMR spectra were recorded at 194.4, 132.3, and 65.6 MHz, respectively, on the General Electric GN-500 spectrometer in 5-mm tubes at 25 °C. The ^{39}K NMR spectra were recorded at 9.26 MHz on the JEOL JNM-FX200 spectrometer in 10-mm tubes at 25 °C. The SRs were prepared in water at a concentration of 8.1 mM and neutralized with $(C_2H_5)_4NOH$ to a pH of 7.0. The alkali-metal chloride salts were added to the SR solutions to a final concentration of 32 mM.

Results and Discussion

Potentiometry. Four polyoxa tetraaza macrocyclic tetraacetic acid derivatives have been prepared by literature methods, with minor modifications. The tetratosyl polyoxa tetraaza macrocycles were fully characterized by NMR spectroscopy, melting points, elemental analysis, and mass spectrometry. These were subsequently detosylated by using 3% Na/Hg amalgam in dry methanol. This method eliminated problems of ether hydrolysis, which would have likely occurred under the more conventional strong acid conditions. The amines were isolated as oils and judged pure by ^{13}C NMR analyses. Carboxymethylation of the macrocyclic amines with bromoacetic acid using standard conditions yielded the targeted polyoxa tetraaza macrocyclic tetraacetic acid derivatives. These were purified by ion-exchange chromatography and judged pure by ^{13}C NMR analyses and potentiometry. We estimate that the presence of impurities greater than 2% would have been detected during analyses of the potentiometric data.

The potentiometrically determined protonation constants of O_3N_4, O_4N_4, O_5N_4, and O_6N_4 are compared to the corresponding values for DOTA[20] in Table I. The protonation constants of the polyoxa tetraaza macrocycles are similar to each other but dif-

(14) Irving, H. M.; Miles, M. G.; Pettit, L. B. *Anal. Chim. Acta* **1967**, *38*, 475.
(15) Cacei, M. S.; Cacheris, W. P. *Byte* **1984**, *5*, 340.
(16) Allinger, N. L. *J. Am. Chem. Soc.* **1977**, *99*, 8127.
(17) Boyd, D. B.; Lipkowitz, K. B. *J. Chem. Educ.* **1982**, *59*, 269.
(18) Wilson, S. *Chemistry by Computer. An Overview of the Applications of Computers in Chemistry*; Plenum Press: New York, 1986.
(19) Spirlet, M.; Rebizant, J.; Loncin, M.; Desreux, J. F. *Inorg. Chem.* **1984**, *23*, 4278.
(20) Delgado, R.; Frausto Da Silva, J. J. R. *Talanta* **1982**, *29*, 815.

Table II. Metal–Ligand Stabilities[a] Calculated from Potentiometric Data at 25 °C

	log K_{ML}	log K_{MHL}	log K_{MH_2L}
$Dy(O_3N_4)^-$	16.7	11.5	5.2
$Dy(O_4N_4)^-$	18.0	11.4	
$Dy(O_5N_4)^-$	16.9	11.1	5.0
$Dy(O_6N_4)^-$	17.6	10.9	
$Dy(DOTA)^-$[b]	24.6		
$Ni(O_3N_4)^{2-}$	18.1	13.4	7.4
$Ni(O_4N_4)^{2-}$	17.6	13.2	7.6
$Ni(O_5N_4)^{2-}$	17.9	13.9	8.3
$Ni(O_6N_4)^{2-}$	18.6	14.0	8.3
$Ni(DOTA)^{2-}$[c]	20.0	11.5	6.5
$Co(O_3N_4)^{2-}$	17.0	12.6	6.9
$Co(O_4N_4)^{2-}$	16.2	12.0	6.8
$Co(O_5N_4)^{2-}$	16.6	12.4	7.2
$Co(O_6N_4)^{2-}$	16.5	12.1	6.8
$Co(DOTA)^{2-}$[c]	20.2	12.1	6.1

[a] The metal–ligand stability constants are defined as K_{ML} = [ML]/[M][L], K_{MHL} = [MHL]/[M][HL], and K_{MH_2} = [MH_2L]/[M][H_2L]. The standard deviation in each value is ±0.1. [b] Reference 21. [c] Reference 20.

ferent from those of DOTA. In each case, the first two protonation constants are lower for the polyoxa tetraaza macrocycles, more like those expected for linear polyamino polycarboxylates.

Stability Constants and Proposed Structures. The thermodynamic stability constants of the four ligands with Dy^{3+}, Ni^{2+}, and Co^{2+} are compared to their respective DOTA complexes[20,21] in Table II. These results show that $Dy(DOTA)^-$ is considerably more stable than the $Dy(O_nN_4)^-$ complexes (average log K_{ML} difference of 7.3). This difference in stability likely reflects the differences in size and rigidity of the metal–ligand complexes. Spirlet et al.[19] have shown that the lanthanide DOTA complexes are unusually rigid and that this rigidity is likely lost when the ring is enlarged by the addition of the polyoxa functionalities. The stability loss due to the increase in ring size[22] is thought to be due to the reduced amine proximity to the metal in the course of the metal–ligand complexation. It would appear that those macrocycles containing an even number of oxygens (O_4N_4 and O_6N_4) form somewhat more stable complexes with Dy^{3+} than do those that contain an odd number of oxygens (O_3N_4 and O_5N_4), although this trend is not preserved in the corresponding Ni^{2+} and Co^{2+} complexes.

The data also show that, unlike $Dy(DOTA)^-$, which remains unprotonated even at pH 3, the $Dy(O_nN_4)^-$ complexes are protonated below pH ≃6. Interestingly, the trioxa and pentaoxa complexes ($Dy(O_3N_4)^-$ and $Dy(O_5N_4)^-$, respectively) undergo two protonations with pK_a's of about 5.8 and 2.8, while the corresponding tetraoxa and hexaoxa complexes ($Dy(O_4N_4)^-$ and $Dy(O_6N_4)^-$, respectively) form only monoprotonated species with pK_a's near 4.9. This again indicates there are some conformational differences between the tri- and pentaoxa complexes and the tetra- and hexaoxa complexes making those $Dy(O_nN_4)^-$ complexes containing an odd number of oxygens protonate more readily. The formation of the MHL species in all four $Dy(O_nN_4)^-$ complexes likely results from protonation of a ring nitrogen, since pK_a's in the range 5–6 are probably too high for a carboxylate protonation. Other workers have shown that basic nitrogens such as those found in these chelates can be protonated, while the remaining donor atoms remain coordinated to the metal ion.[23] The second protonation in $Dy(O_3N_4)^-$ and $Dy(O_5N_4)^-$ to form the MH_2L species could occur at a carboxylate. The species distribution curves for $Dy(O_3N_4)^-$ are presented in Figure 1. These show that very little of the MHL species is present at physiological pH values. Presumably, all four amino and all four carboxylate groups are coordinated to Dy^{3+} above pH ≃7.5 to form an eight-coordinate ML species.

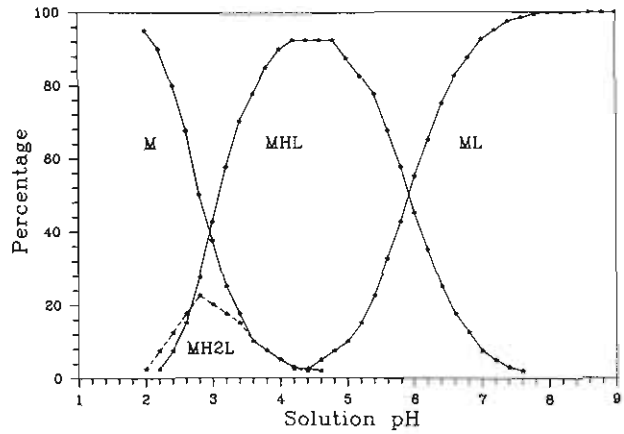

Figure 1. Species distribution curves for $Dy(O_3N_4)^-$.

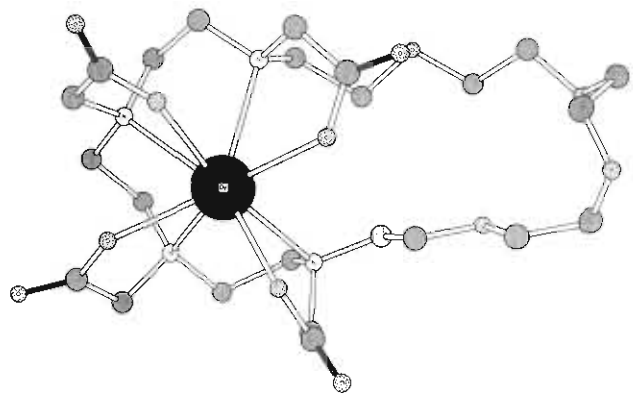

Figure 2. MM2 lowest energy conformation for $Dy(O_4N_4)^-$.

Table III. Ionic Diameters and Hole Sizes (Å)

cation	ionic diameter[a]	crown ether	hole size[b]	Dy(polyoxa tetraazamacrocycle)	hole size[c]
Li^+	1.36	12C4	1.2–1.5	$Dy(O_3N_4)^-$	1.5–1.9
Na^+	1.94	15C5	1.7–2.2	$Dy(O_4N_4)^-$	2.0–2.5
K^+	2.66	18C6	2.6–3.2	$Dy(O_5N_4)^-$	2.4–2.8
Cs^+	3.34	21C7	3.4–4.3	$Dy(O_6N_4)^-$	3.3–4.2

[a] Ionic diameters from ref 24. [b] Crown ether hole sizes from ref 24. [c] Estimated from MMX.

The polyoxa tetraaza macrocyclic ligands also form complexes with Ni^{2+} and Co^{2+} that are only somewhat less stable than their respective complexes with DOTA (average log K_{ML} differences of 2 and 3.6 for Ni^{2+} and Co^{2+}, respectively). This reflects the fact that the Ni^{2+} and Co^{2+} ions are too small for optimal bonding in the cyclododecane ring of DOTA and, hence, do not experience the same drop in stability when the ring is enlarged by addition of the polyoxa functionality as seen in the respective $Dy(O_nN_4)^-$ complexes. $Ni(DOTA)^{2-}$ and $Co(DOTA)^{2-}$ also differ from $Dy(DOTA)^-$ in that both of the transition-metal ion complexes undergo two protonations near pH 4 to form the MHL and MH_2L species. Both protonations are thought to occur at carboxylate sites.[24] The Ni^{2+} and Co^{2+} polyoxa tetraaza macrocyclic complexes also undergo two protonations, but the first occurs at a considerably higher pH (near 7) than for the DOTA complexes. This again suggests the first protonation occurs at a nitrogen (for the reasons stated above for the Dy^{3+} complexes). Further experiments, such as NMR titrations of some diamagnetic complexes, will be necessary to support these proposed protonation sites.

MM2 molecular mechanics calculations on the $Dy(O_nN_4)^-$ complexes allow an estimation of the polyoxa cavity sizes in the series. Table III summarizes these results and compares them

(21) Cacheris, W. P.; Nickle, S. K.; Sherry, A. D. *Inorg. Chem.* **1987**, *26*, 960.
(22) Hancock, R. D.; Martell, A. E. *Comments Inorg. Chem.* **1988**, *6*, 237.
(23) Sawada, K.; Araki, T.; Suzuki, T. *Inorg. Chem.* **1987**, *26*, 1199.
(24) Delgado, R.; Frausto Da Silva, J. J. R.; Vaz, M. C. T. A. *Inorg. Chim. Acta* **1984**, *90*, 185.

Table IV. Paramagnetic Induced Shifts (ppm) for Aqueous Alkali-Metal Cations at pH 7[a]

	Li^+	Na^+	K^+	Cs^+
$Dy(O_3N_4)^-$	0.23	0.12	0.63	2.57
$Dy(O_4N_4)^-$	0.32	0.65	0.63	2.16
$Dy(O_5N_4)^-$	0.18	0.46	0.42	1.92
$Dy(O_6N_4)^-$	0.20	0.42	0.21	1.80

[a] All solutions contained 8.1 mM DyL and 32 mM alkali-metal cation.

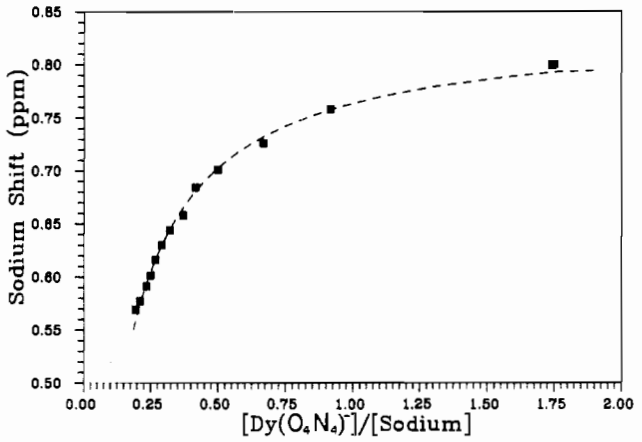

Figure 3. Experimental $^{23}Na^+$ shift induced by 14.3 mM $Dy(O_4N_4)^-$ at pH 7.0. The range of sodium concentrations was 8.2–180 mM. The shifts have been corrected for dysprosium bulk magnetic susceptibility.

with cavity sizes of simple crown ethers. The ionic diameters of four alkali-metal cations are also listed for comparison. It is known that the crown ethers have a binding preference for those alkali-metal cations whose ionic radii best match their cavity size. An estimation of the hole size[25] of the $Dy(O_nN_4)^-$ complexes from MM2 calculations predicts that $Dy(O_3N_4)^-$ may show little preference between Li^+ and Na^+, $Dy(O_4N_4)^-$ should prefer Na^+, $Dy(O_5N_4)^-$ should prefer K^+, and $Dy(O_6N_4)^-$ should prefer Cs^+. An example of the MM2 lowest energy conformation of $Dy(O_4N_4)^-$ is shown in Figure 2. One can see that the macrocyclic ring is bent and the oxygens are staggered to accommodate the lone-pair interactions. It is assumed that, as in the case of crown ether complexes,[22] the polyoxa tetraaza macrocycles will reorient the oxygen lone pairs for best overlap when binding to an alkali-metal cation.

Paramagnetic Shifts. The Dy^{3+}, Ni^{2+}, and Co^{2+} complexes were tested for their ability to induce paramagnetic shifts in the $^{23}Na^+$ NMR resonance of aqueous NaCl at 25 °C and pH 7. Of the complexes studied, only the Dy^{3+} complexes produced measurable shifts in the sodium resonance at the ML/Na^+ concentrations investigated. A comparison of $^{23}Na^+$ shifts observed for solutions containing 8.1 mM DyL and 32 mM Na^+ are found in Table IV. The $^{23}Na^+$ induced shifts were not sensitive to pH in the physiological range. Figure 3 shows the $^{23}Na^+$ NMR shift induced by $Dy(O_4N_4)^-$ (corrected for bulk magnetic susceptibility) when the complex concentration is held constant at 8.1 mM and the concentration of sodium is varied. These data, fit to a 1:1 binding model,[26] give a Na^+ binding constant of 7.59 M^{-1}. This value is similar to constants obtained for Na^+ binding to 15-crown-5 (5.01 M^{-1}) and 18-crown-6 (6.61 M^{-1}) in water[27] and somewhat lower than for Na^+ binding to the anionic shift agent $Dy(TTHA)^{3-}$, as recently reported by Chu et al.[28]

An experiment was also performed to investigate the competition between Na^+ and Ca^{2+} for the polyoxa cavity by titrating a fixed concentration ratio of $Dy(O_4N_4)^-$ and Na^+ with Ca^{2+}. The

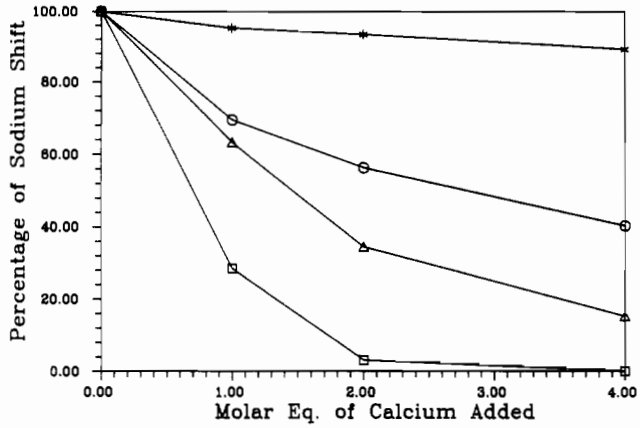

Figure 4. Plots of percent $^{23}Na^+$ paramagnetic shift versus equivalents of Ca^{2+} added per equivalent of SR. Since the initial $^{23}Na^+$ shift and experimental conditions for each SR were quite different, the data are presented normalized relative to the initial shift for each SR in the absence of Ca^{2+}: (✱) $Dy(O_4N_4)^-$; (○) dysprosium(III) triethylenetetraminehexaacetate, $Dy(TTHA)^{3-}$; (△) dysprosium(III) bis(tripolyphosphate), $Dy(PPP)_2^{7-}$; (□) dysprosium(III) 1,4,7,10-tetraazacyclododecane-1,4,7,10-tetrakis(methylenephosphonate), $Dy(DOTP)^{5-}$.

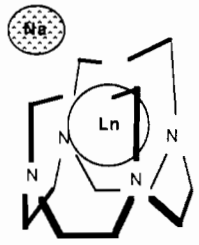

A) $Dy(DOTA)^-$ Type Interaction

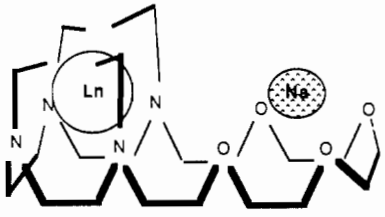

B) $Dy(O_4N_4)^-$ Type Interaction

Figure 5. Schematic models of Na^+ interacting with aqueous shift reagents.

paramagnetic shift observed for the initial solution containing 14 mM $Dy(O_4N_4)^-$ and 8 mM Na^+ was relatively small (0.8 ppm) but decreased to only 0.72 ppm after addition of a total of 56 mM Ca^{2+}. The complete titration results are presented in Figure 4 as percent ^{23}Na shift versus equivalents of Ca^{2+} to total SR concentration. The results are presented in this manner so they may be compared with data from the literature for Ca^{2+} competition with Na^+ for three, more highly charged, anionic SRs.[4,29] As shown, the addition of Ca^{2+} ions to a solution containing one of the more highly charged anionic chelates results in a decrease in the observed $^{23}Na^+$ paramagnetic shift, anywhere from about 40% of the initial value for $Dy(TTHA)^{3-}$ to nearly 100% of the initial shift for $Dy(DOTP)^{5-}$. Ca^{2+} ions do not, however, compete nearly as effectively for the Na^+-binding site on $Dy(O_4N_4)^-$ under similar experimental conditions.

Figure 5 illustrates two possible models for sodium ion interaction with shift reagents. Figure 5A shows the generally accepted

(25) Frensdorff, H. K. *J. Am. Chem. Soc.* **1971**, *93*, 600.
(26) Armitage, I.; Dunsmore, G.; Hall, L. D.; Marshall, A. G. *Can. J. Chem.* **1972**, *50*, 2119.
(27) Izatt, R. M.; Bradshaw, J. S.; Nielsen, S. A.; Lamb, J. D.; Christensen, J. J.; Sen, D. *Chem. Rev.* **1985**, *85*, 271.
(28) Chu, S. C.-K.; Qiu, H. Z.-H.; Springer, C. S., Jr.; Wishnia, A. *J. Magn. Reson.* **1990**, *87*, 287.
(29) Chu, S. C.; Pike, M. M.; Fossel, E. T.; Smith, T. W.; Balschi, J. A.; Springer, C. S., Jr. *J. Magn. Reson.* **1984**, *56*, 33.

model for $Dy(DOTA)^-$, where cations present in solution interact with the negatively charged carboxyl groups. This results is a pseudocontact shift in the sodium resonance, which depends upon the fraction of bound sodium and the average position of the bound Na^+ ion relative to the magnetic symmetry axis of $Dy(DOTA)^-$ (proportional to $(3\cos^2\theta - 1)/r^3$, where θ represents the angle of interaction of the alkali metal with respect to the magnetic symmetry axis of the shift agent and r is the distance between the alkali-metal cation and the lanthanide). In this case, the shift is to low frequency (high field). In this type of interaction, any cation present in solution, such as calcium, can compete for the sodium sites on the shift reagent and thereby reduce the observed $^{23}Na^+$ shift. Figure 5B shows our proposed model of $Dy(O_4N_4)^-$ with a more specific sodium-binding cavity. This polyoxa cavity would not be the appropriate size for most divalent cations; hence, any observed $^{23}Na^+$ shift should be less sensitive to the presence of other competing cations. Experiments performed with $Dy(DOTA)^-$ and $Dy(O_4N_4)^-$ show that the two complexes induce paramagnetic $^{23}Na^+$ shifts in the opposite directions.[30] This indicates that sodium ions indeed bind at geometrically different sites as illustrated in Figure 5.

One possible reason for the small measured shifts might be related to the geometrical interaction of the alkali-metal cations with the $Dy(O_nN_4)^-$ complexes. Bryden et al.[30] state that sodium interacts at an angle less than 54.7° in the lanthanide–DOTA complexes. This is strictly a carboxylate interaction as illustrated in Figure 5A. A logical sodium-binding site based upon our MM2-calculated structures would place the Na^+ ion(s) about 2.3 Å above the carboxylate oxygens, roughly 40° off the 4-fold symmetry axis and about 3.9 Å away from the dysprosium cation. Using our MM2-calculated lowest energy structure for $Dy(O_4N_4)^-$, we estimate a distance of 5.3 Å between the bound dysprosium and a Na^+ atom placed in the center of the polyoxa cavity. This binding site is roughly 106° from the same symmetry axis in the $Dy(DOTA)^-$ portion of the molecule. From the data plotted in Figure 3, a fully bound shift of 8.6 ppm was calculated[25] for the Na^+–$Dy(O_4N_4)^-$ complex. If one assumes the magnetic constants in $Dy(DOTA)^-$ and $Dy(O_4N_4)^-$ are similar in magnitude, the estimated r and θ values for $Dy(DOTA)^-$ may be used to calculate a fully bound shift of −21.2 ppm for the Na^+–$Dy(DOTA)^-$ complex. This indicates that the $^{23}Na^+$ shift for $Dy(DOTA)^-$ is about 2.5 times greater than the corresponding value for $Dy(O_4N_4)^-$ and illustrates the clear advantage of designing a ligand that will bind Na^+ near the symmetry axis of a complex over one which is orthogonal to the symmetry axis.

The small lanthanide-induced shifts for these complexes could also partially result from multiple cation-binding sites. Since the $Dy(O_nN_4)^-$ complexes contain both carboxylate and polyoxa binding sites, the alkali-metal cation shifts may represent a weighted average of an interaction with both sites. If this is true, the magnitude of the shift due to binding to the polyoxa cavity would be partly negated by sodium interactions with the carboxylate sites. However, the very good fit we observe for the Na^+-binding data to a 1:1 binding model suggests that multiple-site binding in these complexes is of little consequence.

Table IV shows the shifts of $^7Li^+$, $^{39}K^+$, and $^{133}Cs^+$ induced by the $Dy(O_nN_4)^-$ complexes. These experiments were performed to evaluate the possible alkali-metal specificity of the individual shift reagents. The results show that in all cases the paramagnetic shifts are small in comparison to the shift range of the individual nuclei.[31,32] The trends show little correlation with cavity size of the individual ligands (Table III). As we increase the cavity size from $Dy(O_3N_4)^-$ to $Dy(O_6N_4)^-$, we see a slight decrease in the overall paramagnetic shifts for ^{39}K and ^{133}Cs. The ^{23}Na NMR shifts are the only ones that agree with the order of size specificity as predicted by the MM2 calculations.

Conclusions

We have designed a series of new ligands that bind paramagnetic cations in the polyaza cavity while leaving an adjacent polyoxa cavity available for binding with alkali-metal cations. However, the dysprosium complexes in this series have somewhat lower thermodynamic stabilities relative to other known SRs. We feel the reduced rigidity of the tetraaza cavity, along with a larger cavity size, lowers the stability of these complexes. MM2 calculations show that the polyoxa cavity sizes of these dysprosium complexes are large enough to accommodate some of the alkali-metal cations, and the NMR experiments indicate that Na^+ has similar affinities for $Dy(O_4N_4)^-$ and crown ethers in aqueous solution. Although this SR does appear to have a greater selectivity for Na^+ over Ca^{2+}, the paramagnetic shifts induced by the $Dy(O_nN_4)^-$ complexes in alkali metal cation NMR resonances are relatively small. This makes it unlikely these new complexes will be useful as SRs for in vivo NMR studies. It is also possible that the $Dy(O_nN_4)^-$ chelates may act as ionophores in some cells, since complexes with Na^+ and K^+ would be electrically neutral. However, we anticipate that future development of new shift agents similar to $Dy(O_4N_4)^-$ which have reduced divalent cation affinities but which also have higher lanthanide stability constants may ultimately allow a wider variety of in vivo $^{23}Na^+$ NMR studies.

Acknowledgment. We are grateful for financial support of this research from the Meadows Foundation and the Robert A. Welch Foundation (Grant AT-584). We thank John Sibert and Professor Jonathan Sessler of the University of Texas at Austin for providing us with an initial sample of the O_4N_4 macrocycle in the free amine form. Jonathan Sessler wishes to acknowledge National Institutes of Health Grant GM R0136384 for his portion of the work. We also thank Drs. Flavio Chavez Lopez and Erno Brucher for their help with synthesis and stability constant determinations, respectively.

(30) Bryden, C. C.; Reilley, C. N.; Desreux, J. F. *Anal. Chem.* **1981**, *53*, 1418.

(31) Popov, A. I.; Lehn, J. In *Coordination Chemistry of Macrocyclic Compounds*; Melson, G. A., Ed.; Plenum Press: New York, 1979; Chapter 9.

(32) Detellier, C. In *NMR of Newly Accessible Nuclei*; Laszlo, P., Ed.; Academic Press: New York, 1983; Vol. 2, Chapter 5.